Industrial Crops & Products 187 (2022) 115299

Contents lists available at ScienceDirect

Industrial Crops & Products

journal homepage: www.elsevier.com/locate/indcrop

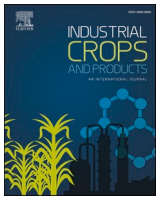

Poly (itaconic acid) functionalized lignin/polyvinyl acetate composite resin with improved sustainability and wood adhesion strength

Tuhin Ghosh [a], Timo Elo [a], Vijay Singh Parihar [b], Pralay Maiti [c], Rama Layek [a,*]

[a] LUT University, School of Engineering Science, Department of Separation Science, Mukkulankatu 19, 15210 Lahti, Finland
[b] Biomaterials and Tissue Engineering Group, BioMediTech, Faculty of Medicine and Health Technology, Tampere University, Finland
[c] School of Materials Science and Technology, Indian Institute of Technology (Banaras Hindu University), Varanasi 221005, India

ARTICLE INFO

Keywords:
Poly (itaconic acid)-functionalized lignin
Sustainability, Poly(vinyl acetate) emulsion
Composite
Adhesion strength

ABSTRACT

In this current scenario, there is a broad range of use of resins in both domestic and industrial applications. Especially the importance of resins for adhesive in the wood industry is inevitable. But most of the commercially available resins for adhesive application are prepared of formaldehyde or fossil fuel-based resources which possess serious health issues. Henceforth, development of environmentally friendly resin from renewable resources through a cost-effective technique is a challenging task. Motivated by these facts and prospects, we present a novel technique for addressing non-renewability difficulties while also improving adhesive strength of the material. In this study, lignin-based composite resin with enhanced sustainability and adhesion strength have been achieved by a simply mixing of high concentration of poly (itaconic acid)-functionalized-lignin (P(IA)-f-Lignin) and aqueous emulsion of polyvinyl acetate. The P(IA)-f-Lignin was synthesized by in-situ free radical polymerization of partly neutralized IA in the presence of aqueous lignin dispersion at 90 °C using ammonium persulfate as initiator. The formation of P(IA)-f-Lignin was confirmed by Fourier transform infrared spectroscopy (FTIR), X-ray photoelectron spectroscopy (XPS), nuclear magnetic resonance (NMR), field emission scanning electron microscope (FESEM) and thermogravimetric analysis (TGA). Here, we have been fabricated 20, 30, 40, 50, and 60 wt% of P(IA)-f-Lignin containing composite resin with desired amount of aqueous emulsion of polyvinyl acetate (PVAc). The changes in physico-chemical interactions were established by FTIR analysis. Various properties like viscosity, thermo-stability, and adhesive properties of all the formulated composite resin were inspected thoroughly. The composite containing 40 wt% of P(IA)-f-Lignin shows excellent improvement of adhesion strength from 3.32 ± 0.12 MPa to 7.83 ± 0.45 MPa. These fabricated composite resin with a high concentration of bio-based P(IA)-f-Lignin content and strong adhesion strength is very promising for fabrication of biobased adhesives with improved sustainability.

1. Introduction

From the primitive beginnings to the present time, resins play a vital role in day-to-day life and their use is constantly growing in packaging, furniture, sealant, automotive and decoration industries (Dinte and Sylvester, 2018; Khan et al., 2013). Moreover in the last few decades, the wood industry flourishes significantly due to the rapid modernization of civilization. The range of applications in the wood industry is gigantic which includes wood bonding, furniture manufacturing, installation of wooden flooring, roof decking and wall sheeting etc (Todorovic et al., 2021). Henceforth, there is a huge craving of resin for adhesives, and it becomes a multi-billion-dollar business. As a result, there is a lot of research being done at both the academic and industrial levels to find a new generation of resin that is mechanically robust for use in adhesive applications.

Among various well-known wood adhesives, formaldehyde-based resins (FBRs) like phenol-formaldehyde, melamine-formaldehyde and urea-formaldehyde are the most important due to its low cost, fast curing process and effective strength (Jiang et al., 2018; Pei et al., 2020; Rana et al., 2021a, 2021b, 2021c). Prior art literatures advocate the presence of a huge number of research article on the development of FBRs. But the use of FBRs is strictly prohibited due to the emission of carcinogenic formaldehyde during manufacturing and use as well as the leaching tendency of the unreacted formaldehyde (through the

* Corresponding author.
E-mail address: rama.layek@lut.fi (R. Layek).

https://doi.org/10.1016/j.indcrop.2022.115299
Received 4 May 2022; Received in revised form 28 June 2022; Accepted 28 June 2022
Available online 7 July 2022

hydrolytic process) during its service life (Li et al., 2018). From prior art study it was found that the amount of formaldehyde emission reach ≥ 0.8 ppm whereas the detrimental effect on human health (e.g., rhinitis, irritation of throat, eye, and respiratory tracks, cancer etc.) starts from 0.4 ppm (Salthammer et al., 2010). The hazardous problems with FBRs reduce their use and accelerated up the development of non-formaldehyde-based adhesives. In this milieu, two-component epoxy systems, polyurethane resins, and poly(vinylacetate) (PVAc) are widely used as promising alternatives to FBRs (Li et al., 2018; N. Zhang et al., 2021). Two-component epoxy resins exhibited strong bonding ability between wooden substrates, but these systems also involve severe drawbacks like contamination problem and uneven mixing of two-compartment systems, high-temperature curing, brittle nature of the cured adhesives as well as non-renewability and non-biodegradability (Baş and Sancaktar, 2020; Todorovic et al., 2021). This problem is addressed by flexible polyurethane (PU)-based resins but most of the commercialized PU resins are solvent-borne and synthesized from hazardous raw materials like diisocyanates (Todorovic et al., 2021). Henceforth, the usage of PVAc-based resins is now the most worthwhile answer to the aforementioned difficulties due to its non-toxic nature, low cost, biodegradability along with the waterborne nature makes it environmentally friendly among all the existing wood bonding adhesives (Chaabouni and Boufi, 2017; Kaboorani and Riedl, 2012; Zhang et al., 2020).

Despite these advantages, PVAc resin don't have sustainability as it is derived from non-renewable petroleum-derived resources. Usually, it forms a strong adhesive bond with porous surfaces like wood and paper, however its adhesive strength is restricted by the mechanical properties of the polymeric resin. To improve the physical and mechanical properties of PVAc resin various types of additives have been reinforced into the PVAc matrix. As for example, Khan et al. prepared a series of graphene-PVAc adhesives by altering the concentration of graphene (Khan et al., 2013). Maksimov et al. have shown the effect of physico-mechanical properties of PVAc composite with different concentration of carbon nano tubes (Maksimov et al., 2010). Kaboorani and Riedl prepared a series of nano clay-PVAc adhesives by judicial integration of nano clay into PVAc resin (Kaboorani and Riedl, 2011). They also incorporated aluminum oxide nanoparticles to improve the bonding strength of PVAc adhesive in moist condition and in elevated temperature (Kaboorani and Riedl, 2012). Though it is reported in the above-mentioned articles that the adhesive properties of PVAc-based composite resins enhanced marginally with the integration of nano material as additives, however the integrated nano additives don't have sustainable resources and therefore cannot enhance the sustainability of PVAc resin. Currently, the sustainability of the polymeric additives is getting considerable attention for the development of sustainable products for a green future. Among various types of sustainable bio-additives, the lignocellulosic bio-additives such as nanocellulose and lignin are very promising bio-additives to enhance the sustainability of the polymer composites (Rana et al., 2021a, 2021b, 2021c; Song et al., 2022; Uppal et al., 2022; Kumar et al., 2022). In this connection, there are few reports of the integration of bio-based green additives to improve adhesive characteristics of the PVAc resin. Chaabouni and Boufi, Suevos et.al, formulated a series of adhesives by simply mixing PVAc dispersion with various concentration of cellulose nanofibrils as bio-additives (Chaabouni and Boufi, 2017; López-Suevos et al., 2010). Kaboorani et al. formulated different compositions of PVAc composite adhesive by integrating different concentration (1–3 wt%) of nanocrystalline cellulose as bio-additives (Kaboorani and Riedl, 2011). Wen et al. examined the adhesive bond strength of PVAc composite resins with cellulose nanofibrils based bio-additive and it increased with increased of cellulose nanofibrils concentration (Jiang et al., 2018). Generally, very low amount of nanocellulose-based additive is integrated into PVAc resin to improve the wood adhesive property. Though it can moderately improve the wood adhesion property, but it has a high preparation cost and cannot enhance the sustainability of the PVAc composite resin significantly due to the presence of very low amount of nanocellulose.

Currently, lignin is considered a promising sustainable and cost-effective bio-additives for polymeric resin as it is produced on a huge scale as a byproducts in the paper and pulp industry (Kaur et al., 2021). Lignin is the second most prevalent biopolymer, with a chemical structure containing repetitive units of multi aromatic phenols connected by complicated ether-linkages (Zhang et al., 2020; Z. Zhang et al., 2021). But, lignin's incompatibility with other components due to its highly branched aromatic structure is the main problem and it limits the application of lignin as bio-additives. To exploit the properties of lignin as bio-additives and enhance its compatibility with polymeric resin, the functionalization of lignin with a suitable functional group is essential. Previous reports claim the presence of various phenol treated lignin-polyvinylpyrrolidone adhesive, lignin-epoxy adhesive etc (Gong et al., 2020; Li et al., 2018; Zhang et al., 2018). But the use of toxic chemicals throughout the modification and poor mechanical property restricts its future possibilities. Prior art literatures claim the synthesis of lignin-PVAc-based resin as coating (N. Zhang et al., 2021; Zhang et al., 2020). Shu et al. used maleic anhydride grafted-lignin and further functionalized with PVAc to improve the properties of poly(lactic acid) (Shu et al., 2021). Zhang et al. prepared lignin-vinyl acetate from aminated lignin and further copolymerize with vinyl acetate in different wt % (Zhang et al., 2020). Multiple steps of lignin modification, use of formaldehyde and very low bio-content confine the sustainability of the final product and moreover, the adhesive properties of the materials have not been explored. Despite the limited advancements in functionalized lignin-based resin, there have been no reports of PVAc composite resins containing significant amounts of functionalized lignin as bio-additives. Nevertheless, this study is crucial for improving the sustainability and compatibility of PVAc composite resin.

Herein, for the first time, we report a PVAc composite resin with a high concentration of biobased poly (itaconic acid) functionalized lignin (P(IA)-f-Lignin) via tailoring the surface chemistry of lignin. At first, we successfully synthesized a novel P(IA)-f-Lignin via in-situ polymerization of partially neutralized itaconic acid in presence of aqueous dispersion of lignin. The main objective of this work is to investigate the compatibilization chemistry and reinforcing performance of P(IA)-f-Lignin into PVAc resin as well as explore the sustainability and scope of bioeconomy of lignin. P(IA) has chosen due to the biobased resource of IA monomer (a by-product from the sugar industry), easy availability and low cost (Rezania et al., 2019). Beside this P(IA) contains bifunctional carboxylic acid group in each monomer unit that can enhance the compatibility of lignin with the aqueous emulsion of PVAc (Sánchez-Valdes et al., 2012). The composite resins contain a high concentration of biobased P(IA)-f-Lignin of 20, 30, 40, 50 and 60 wt% with respect to PVAc. The judicial integration of biobased P(IA)-f-Lignin additives enhance the wood adhesion strength remarkably compared to pure PVAc resin. Hence, P(IA)-f-Lignin not only enhance wood adhesion strength but also enhances the sustainability P(IA)-f-Lignin/PVAc resin compared to pure PVAc resin. The physical, thermal, and mechanical properties of the composite resins were examined and correlated with the structure property relationship of the P(IA)-f-Lignin/PVAc resin composite. To evaluate the superiority of the P(IA)-f-Lignin/PVAc resins the wood adhesion strength has been compared with prior art literatures. We observed that the PVAc@P(IA)-f-Lignin composite resin has significantly greater adhesive properties than pure PVAc resin.

2. Experimental

2.1. Materials

Vinyl acetate, sodium dodecyl sulfate, sodium bicarbonate, ammonium persulfate (APS), poly(vinyl)alcohol (PVA) (M_W ~ 13,000–23,000, 87–89 % hydrolyzed), itaconic acid (IA) were procured from Sigma and used as received. N,N-Dimethylformamide was

purchased from Sigma and used as received. Kraft lignin (hydroxyl value: 6.07 mmol/g, acid value: 0.49 mmol/g) was obtained from UPM Biochemicals (Finland) and grinding thoroughly using mortar and pestle before use.

2.2. Methods

2.2.1. Synthesis of P(IA)-f-Lignin

The initial synthesis procedure includes the 40 % neutralization of IA using a calculated amount of potassium hydroxide. Briefly, 10 g of IA and 15 mL of water were taken in a 100 mL beaker. Then the mixture was heated gently at 80 ℃ for 10 mins under magnetic stirring. In another beaker, 3.45 g of KOH was dissolved in 5 mL of water. Afterwards, the KOH solution was added dropwise to the solution of IA for neutralization. Here, 40 % neutralized IA was used for the synthesis of P(IA)-f-Lignin. In a two neck round bottom (RB) flask, 5 g of lignin and 20 mL of water were taken and ultrasonicated for a period of 30 min. Then the neutralized IA solution was added to the RB flask under stirring condition. Afterwards, 3 wt% (w.r.t lignin) APS was added to the RB flask and heated gently under N_2 atmosphere at 80 ℃ for 4 h under continuous magnetic stirring. After completion of the reaction, the obtained reaction mixture was filtered using a Whatman filter paper and washed simultaneously to remove the free P(IA) and unreacted itaconic acid monomer units. Then the residue was dried under ambient temperature and grinding thoroughly before characterization and its further use. The synthesis of P(IA)-f-Lignin has been shown in Scheme 1 for a better understanding.

2.2.2. Preparation of PVAc-based resin containing P(IA)-f-Lignin

Emulsion polymerization technique as described by Wang et al. was used to formulate the PVAc emulsion using PVA as an emulsion stabilizer (Wang et al., 2012). After that 20, 30, 40, 50 and 60 wt% of P(IA)-f-Lignin was blended with the aqueous emulsion of PVAc as shown in Scheme 2.

A homogeneous stable dispersion of PVAc@P(IA)-f-Lignin was observed after 15 mins of blending using high-speed mixer and corresponding compositions are encoded as PVAc-P(IA)-f-L-20, PVAc-P(IA)-f-L-30, PVAc-P(IA)-f-L-40, PVAc-P(IA)-f-L-50 and PVAc-P(IA)-f-L-60. The prepared formulations are used directly for adhesion test and further characterization. Here, it is pertinent, to mention that first three compositions (20, 30 and 40 wt%) are characterized in detail whereas other two compositions (50 and 60 wt%) are formulated to understand the change in mechanical property in higher loading of P(IA)-f-Lignin.

2.2.3. Characterization

PerkinElmer Spectrum One FTIR Spectrophotometer (PerkinElmer, Waltham, MA) in attenuated total reflection (ATR) mode was used to characterize the presence of different functional groups. NMR spectra of lignin and functionalized lignin were recorded using JEOL-500 MHz instrument (SCZ500R, JEOL Resonance, Japan) in DMSO-d6 as solvent. The surface zeta potential was measured with the Zetasizer Nano ZS, Malvern, UK at 25 °C using disposable folded capillary DTS1070 cells. The chemical composition of the lignin and P(IA)-f-Lignin was scrutinized by XPS (Model No. PHI 5000 Versa Probe III instrument) and all the obtained XPS data were processed using Origin Pro 21 software. Thermogravimetric analysis (TGA) was carried out using TGA-Q-500 (TA Instruments, New Castle, DE, USA) instrument over the temperature range of 25–800 °C with a temperature ramp of 10 °C/min under ultrapure N_2 atmosphere. All rheological experiments were performed on a rotational rheometer (Discovery HR-2, TA Instruments Inc., USA) in parallel plate geometry (12 mm plate).

Adhesion properties of the prepared formulations were measured using lap shear test method in both dry and wet-redry state. Wooden blocks of particular size (length: 100 mm × width: 20 mm × thickness: 9 mm) were used for adhesive bonding test. After applying glue to the wooden blocks, they are allowed to dry completely at room temperature for 12 h. For 'redry state' test, the glued wooden blocks after complete drying (12 h) were immersed in water for 6 h. The temperature of the water was kept constant at 20 ± 1 °C during the immersion period. Then the wooden blocks were left in ambient temperature to remove the water. Afterwards, the lap-shear test was performed using a Universal tensile test (UTM) instrument (Shimadzu, AG-IC 100 kN) with a cross-head speed of 50 mm/min. Shear strength (T in N/mm^2 or MPa) was calculated by using the following equation.

$$T = F_{max}/l.b \quad (1)$$

Where F_{max} denotes the maximum force at break, l denotes the length of the tested bonded surface, and b denotes the width of the bonded surface. For each adhesive composition, the average results of five samples were represented.

Morphology of lignin, P(IA)-f-Lignin and the mechanically fractured wooden surfaces were inspected by Field-Emission Scanning Electron Microscope (FE-SEM, JSM-7900F, Jeol).

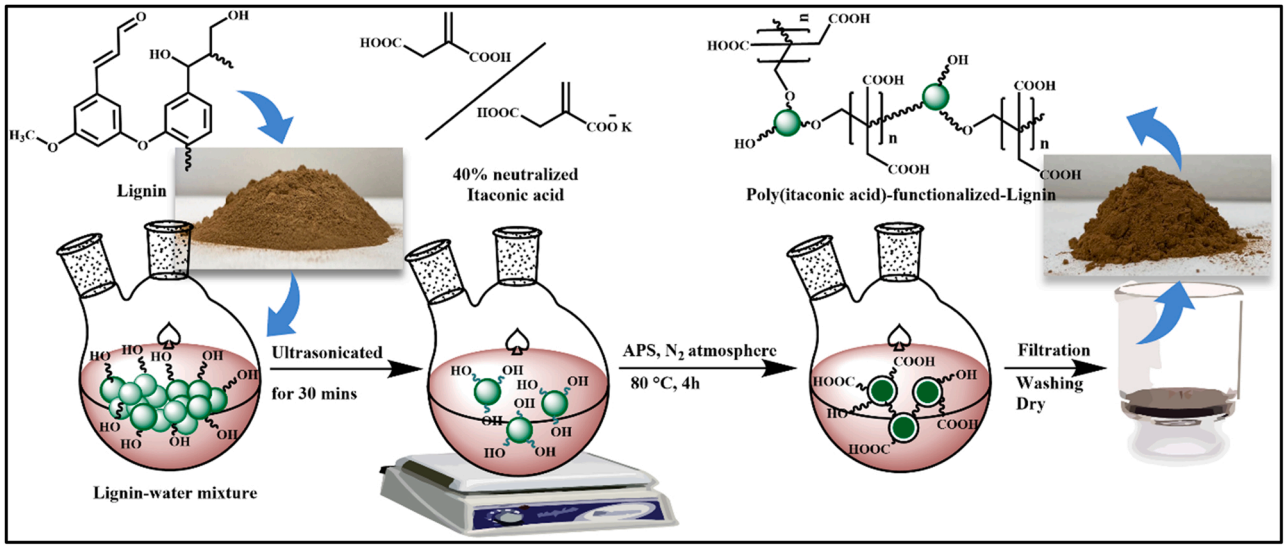

Scheme 1. Schematic representation for the synthesis of P(IA)-f-Lignin.

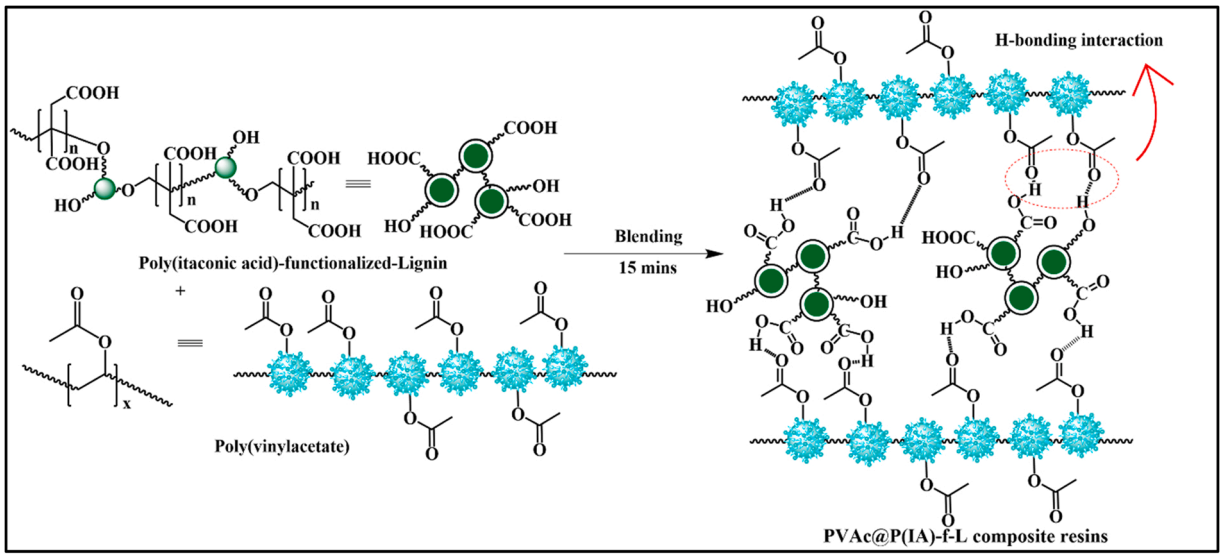

Scheme 2. Schematic representation of the formation of PVAc@P(IA)-f-L composite resin.

3. Result and discussion

3.1. Synthesis of P(IA)-f-Lignin

A partially neutralized aqueous solution of IA was used to synthesize P(IA)-f-Lignin. Generally, at room temperature IA shows poor solubility in water. But the solubility increases with the increase of temperature. Moreover, the rate of polymerization of IA is very low and takes longer time to form low molecular weight P(IA) chains. From a previous report, it is evident that the rate of polymerization will be faster if the amount of neutralization is increased (Bednarz et al., 2015). Henceforth, to improve the dispersion behavior as well as to increase the rate of polymerization, 40 % neutralized IA was used. In the next step, in-situ radical polymerization of neutralized IA was employed for

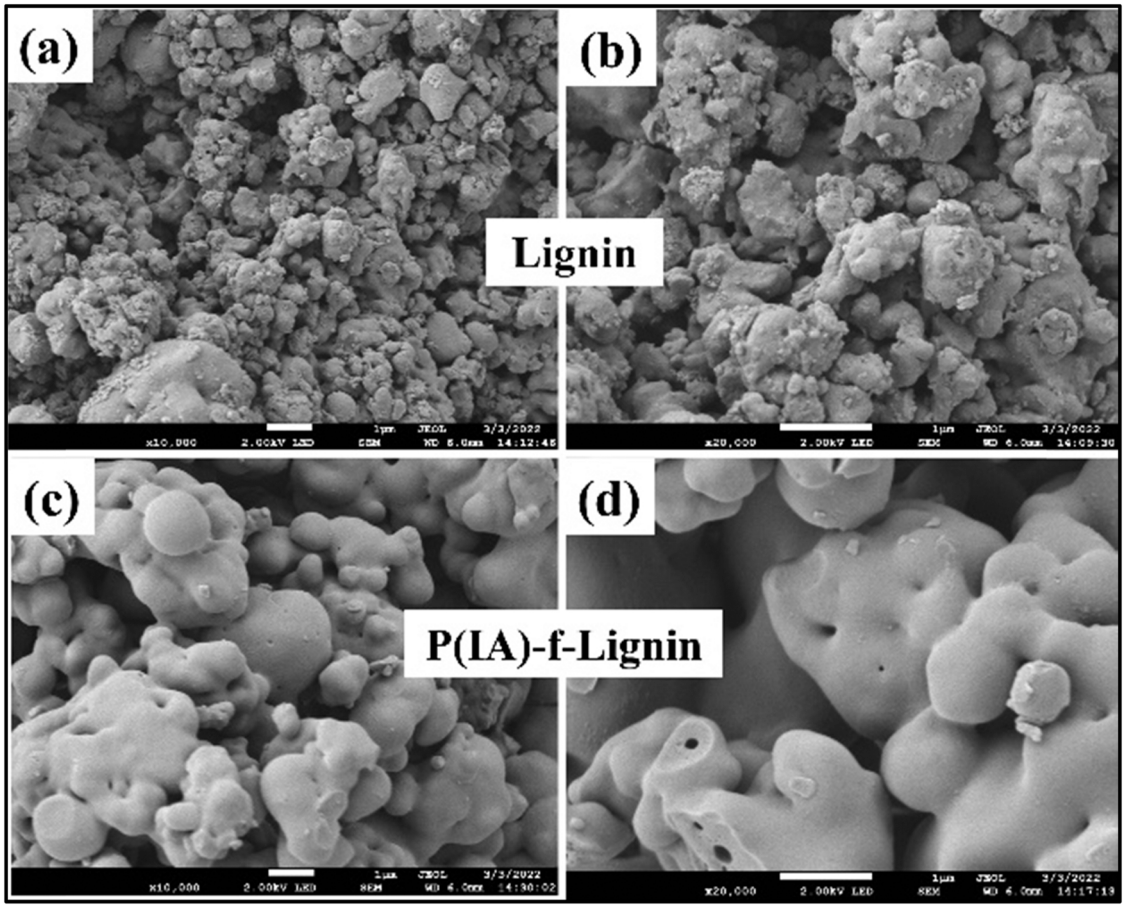

Fig. 1. FESEM images of lignin (a, b) and P(IA)-f-Lignin (c, d) in different magnification.

functionalization process of lignin. The complex structure of lignin contains several aromatic/aliphatic -OH groups. These -OH groups of lignin generate reactive Lignin-O• radicals from where P(IA) chains are grown during is-situ radical polymerization of IA. The structural and morphological changes occurred after the functionalization of lignin was confirmed by checking the dispersion behavior as well as with the help of scattering (DLS), spectroscopic (FTIR NMR, FESEM) and gravimetric techniques (TGA).

Lignin is a complex molecule and shows poor dispersion behavior in water. Heterogenous solution is observed even after sonication. But after modification with P(IA), a homogeneous dispersion is observed. Change in dispersion behavior is due to the increasing polar functional groups of lignin. This is further supported by the evaluation of zeta potential. From the zeta potential measurement, it is evident that lignin shows zeta potential of − 15.5 mV whereas after modification zeta potential decreases to − 36 mV. Inclusion of carboxyl group (especially oxygeneous functional groups) after modification with P(IA) is the reason behind such improved dispersion behavior (Yang and Gunasekaran, 2013).

However, for better understanding the change in morphology was investigated using FESEM analysis as shown in Fig. 1. The surface of the lignin particles is exceedingly rough before functionalization, as shown in the images (Fig. 1. a and b), while the surface of lignin is smooth after functionalization with P(IA). From the presented images (Fig. 1. c and d) it is clear that globular lignin particles are coated with P(IA). This could be due to the covalent functionalization of P(IA) from lignin particles during in-situ polymerization, which leaves a wrap on the surface of the lignin particles and enhance the smoothness of P(IA)-f-Lignin.

3.2. Structural characterization of P(IA)-f-Lignin

Change in functionalities before and after modification were scrutinized with the help of FTIR spectra (Fig. 2.a). In lignin the characteristic bands at 3406, 1706, 1366, 1217 and 1125 cm^{-1} correspond to hydrogen bonded O-H (phenolic and aliphatic O-H) stretching, carbonyl stretching of unconjugated ketone, O-H deformation, phenolic C-O stretching and C-O stretching of secondary alcohols, respectively (Crouvisier-Urion et al., 2019; Yan et al., 2015; Zong et al., 2018). The above-mentioned bands underwent a significant amount of red shift in P(IA)-f-Lignin. The O-H stretching band for phenolic and aliphatic groups appears at 3380 cm^{-1}, carbonyl stretching of unconjugated ketone appears at 1702 cm^{-1}, O-H deformation appears at 1363 cm^{-1}, respectively. Such kind of red shift in the FTIR spectra (Fig. 2. b and c) correspond to the generation of strong H-bonding in lignin after chemical functionalization with P(IA) (Wang et al., 2019). Noticeably, the intensity of the -OH stretching frequency increases significantly compared to the -OH stretching frequency of lignin. This is due to inclusion of additional carboxyl -OH group due to functionalization process. Moreover, the asymmetric and symmetric stretching vibration of C-H bond (2933 and 2840 cm^{-1}), aromatic skeleton vibrations (1598–1593, 1511–1509 and 1425–1423 cm^{-1}), breathing vibrations of syringyl ring along with C-O stretching (1264 cm^{-1}), in plane (1028 cm^{-1}) and out of plane (842 cm^{-1}) vibrations of aromatic C-H bond are common in the FTIR spectra of both lignin and P(IA)-f-Lignin (Crouvisier-Urion et al., 2019; Panesar et al., 2013). These results support the successful functionalization of lignin.

Further, the change in chemical characteristics of lignin and P(IA)-f-Lignin was investigated thoroughly using XPS analysis and the deconvoluted spectra of C 1s and O 1s are shown in Fig. 3. a–d. The deconvoluted spectrum of C 1s (Fig. 3. a) revealed the presence of signature peaks for kraft lignin, centered at 284.5 eV, 285.7 eV and 288.6 eV correspond to the binding energy of C—C/C═C, C—O—C/C—OH and C═O/OH—C═O bonds, respectively. Moreover, three peaks found in the deconvoluted spectrum of O 1s (Fig. 3. b) at binding energy of 531.4 eV, 532.5 eV and 533.3 eV also support the presence of Ph═O/Ph—C═O/O—O, C═O/O═C—OH and Ph—OH/C—O bonds, respectively (Myint et al., 2016; Zhang et al., 2020). Exactly, similar kind of functionalities along with their respective binding energy peaks are also found in the deconvoluted C 1s and O 1s spectra (Fig. 3. c and d) of P(IA)-f-lignin. The carbon/oxygen ratio for lignin and P(IA)-f-Lignin also changes from 2.89 to 3.26. This increasing trend in carbon/oxygen ratio corresponds to surface functionalization of P(IA) on the surface of lignin. Presence of corresponding functionalities resembles with the FTIR data.

^{1}H NMR technique was employed to support the efficient functionalization of P(IA) into lignin and the corresponding NMR spectra were presented in Fig. 4. It was revealed from the ^{1}H NMR spectrum (Fig. 4. a) investigation that the chemical shift values at 0.6–2.3 ppm, 3.55–3.89 ppm, 4–5.8 ppm, 6–7.5 ppm, 7.5–9.5 ppm correspond to the protons of saturated aliphatic groups, methoxy protons, aliphatic protons of unsaturated/γ-CH_2-O-/α-CH-O- groups, aromatic and phenolic

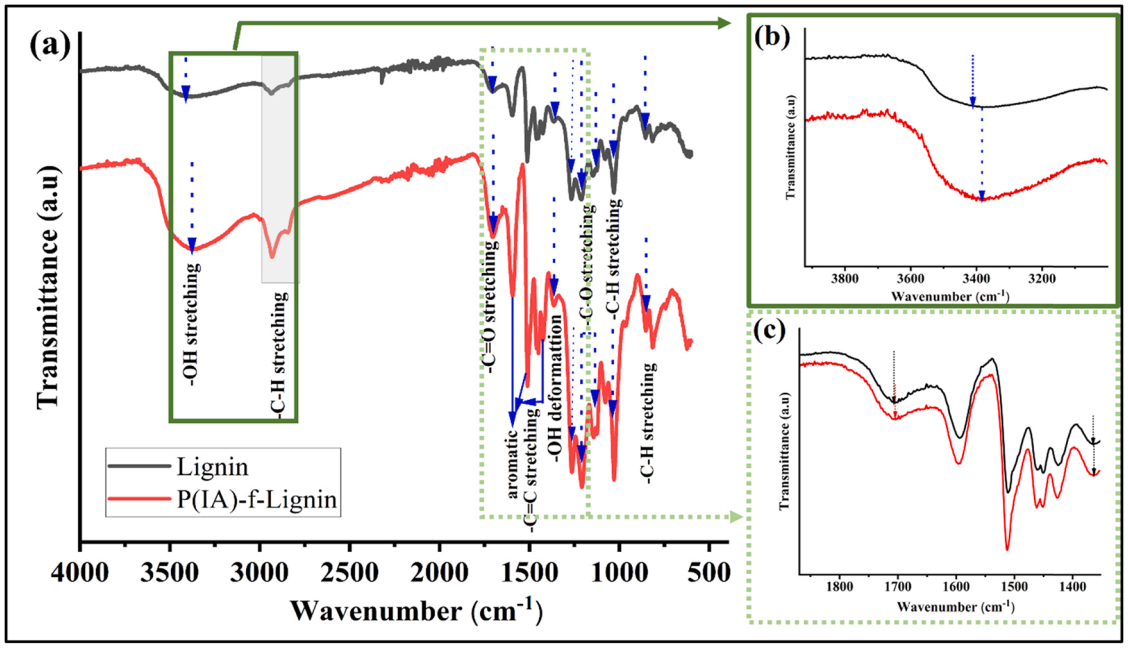

Fig. 2. (a) FTIR spectra of lignin and P(IA)-f-Lignin and (b & C) are the expanded region of the spectra.

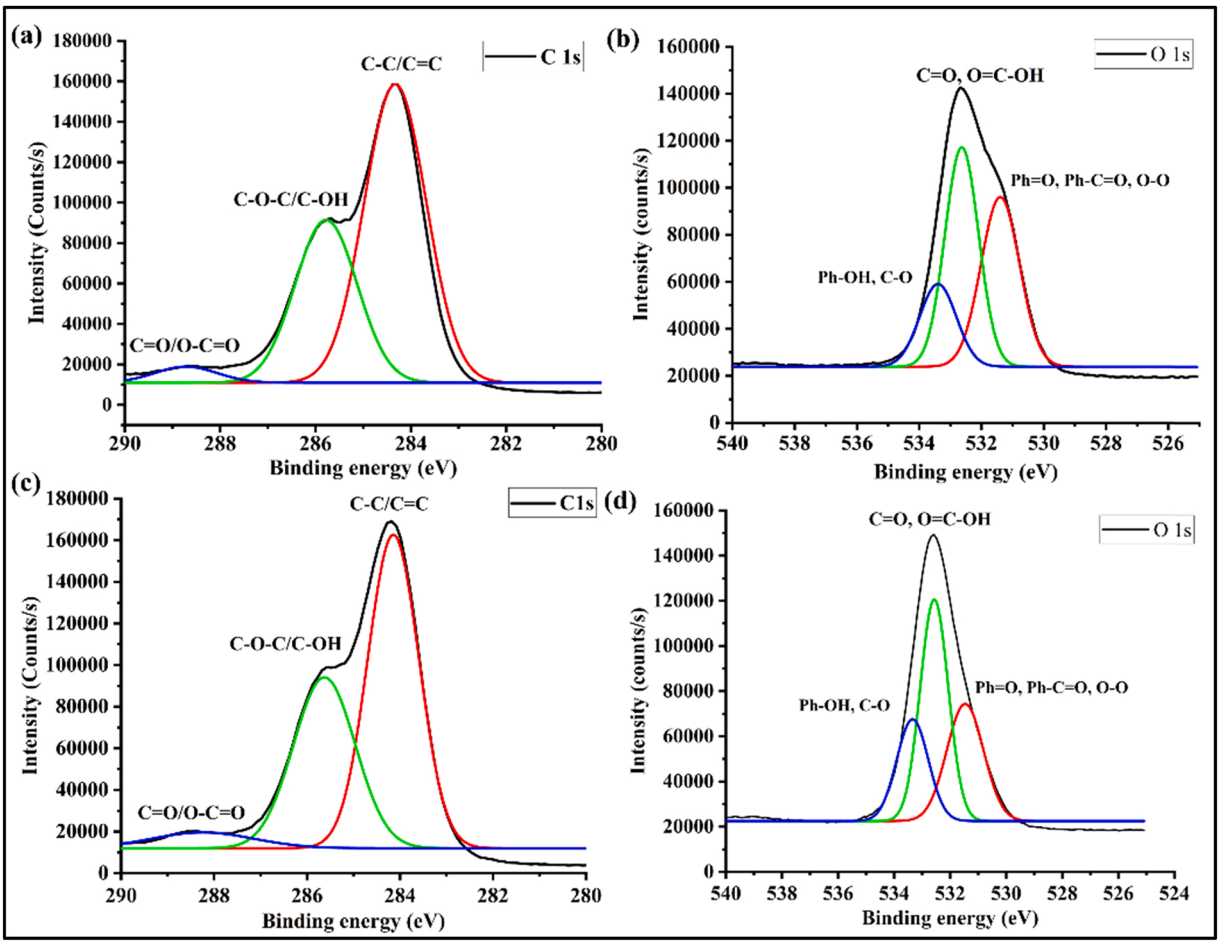

Fig. 3. XPS spectra of C1s and O1s of lignin (a & b) and P(IA)-f-lignin (c & d).

protons, respectively (Kollman et al., 2021). Whereas slight changes are observed in the spectrum (Fig. 4. b) of lignin after modification with P (IA). The characteristic signals for the P(IA) are observed at $\delta = 1.24$ ppm and 3.21 ppm which correspond to the methylene protons of main polymeric chain and methylene protons of -CH_2-COOH group, respectively (Cottet et al., 2021; Rezania et al., 2019). A very weak signal at $\delta = 12.3$ ppm corresponds to the protons of -COOH group in P (IA). Moreover, other peaks found in the NMR spectrum of P (IA)-f-Lignin are resembles with the NMR spectrum of lignin.

TGA was applied to evaluate the impact of P(IA) functionalization on the thermal degradation profile of lignin. Weight loss curves and their derivative thermograms are represented in Fig. 5. Thermograms of lignin and P(IA)-f-Lignin revealed a multi-step degradation pattern across a wide temperature range, and the results are consistent with previous research (Yan et al., 2015; Yu et al., 2012). In both the curves the degradation starts with the evaporation of physically absorbed water molecule in the temperature below 100 ℃. In lignin, three different kinds of degradation are observed which includes a shoulder peak in the temperature range of 170–280 ℃ (peak degradation temperature (PDT): 197 ℃), a sharp second degradation peak in the temperature range of 280–470 ℃ (PDT: 414 ℃) followed by a third degradation peak in between the temperature range of 470–720 ℃ (PDT: 557 ℃). The first degradation corresponds to the degradation of most thermolabile functional groups (ether linkages, ketones, methoxyls, alcoholic -OH etc.) present in the structure of lignin. The second degradation assigns to the cleavage of C—C bond followed by depolymerization of lignin into smaller fragments (such as aromatic phenols). In third step of degradation, such kind of smaller fragments underwent carbonization reaction and formed thermally inert char layer (Manara et al., 2014). But after functionalization with P(IA), some changes are found in degradation profile. In the first degradation region, P(IA)-f-Lignin showed enhanced thermal stability compared to lignin with a PDT of 265 ℃. Such kind of behavior might be due to the reduction of -OH functional groups in lignin after radical polymerization with P(IA). But the intensity of the degradation increases with the upsurge in temperature, which associates to the degradation of carboxylic groups in the structure of P(IA). In the second step of degradation, C-C bonds cleavage/depolymerization occurs both in lignin and P(IA), leading to a broad degradation intensity compared to lignin. Eventually, Due to such broad degradation behavior, third step of degradation started before completion of second step of degradation (Tomić and Filipović, 2004). Furthermore, from the difference in weight residue% at 600 °C, it was found that 8 wt% of P(IA) was grafted to the lignin.

3.3. Preparation of PVAc@P(IA)-f-L composite resins

The compositions of PVAc adhesive with different wt% of P(IA)-f-Lignin were prepared by simple blending technique. It is important to mention that good and stable dispersion of P(IA)-f-Lignin in PVAc is necessary to obtain optimum property.

3.4. Characterization of PVAc@P(IA)-f-L composite resins

Presence of different type of functional groups are confirmed from the displayed FTIR spectra in Fig. 6. a. Characteristic bands in PVac at 2929 and 2848, 1728, 1371, 1226–1080 cm^{-1} correspond to the asymmetric and symmetric stretching of sp^3 hybridized C—H bond, carbonyl (-C═O) stretching of acetate, -O–H deformation, -C–O

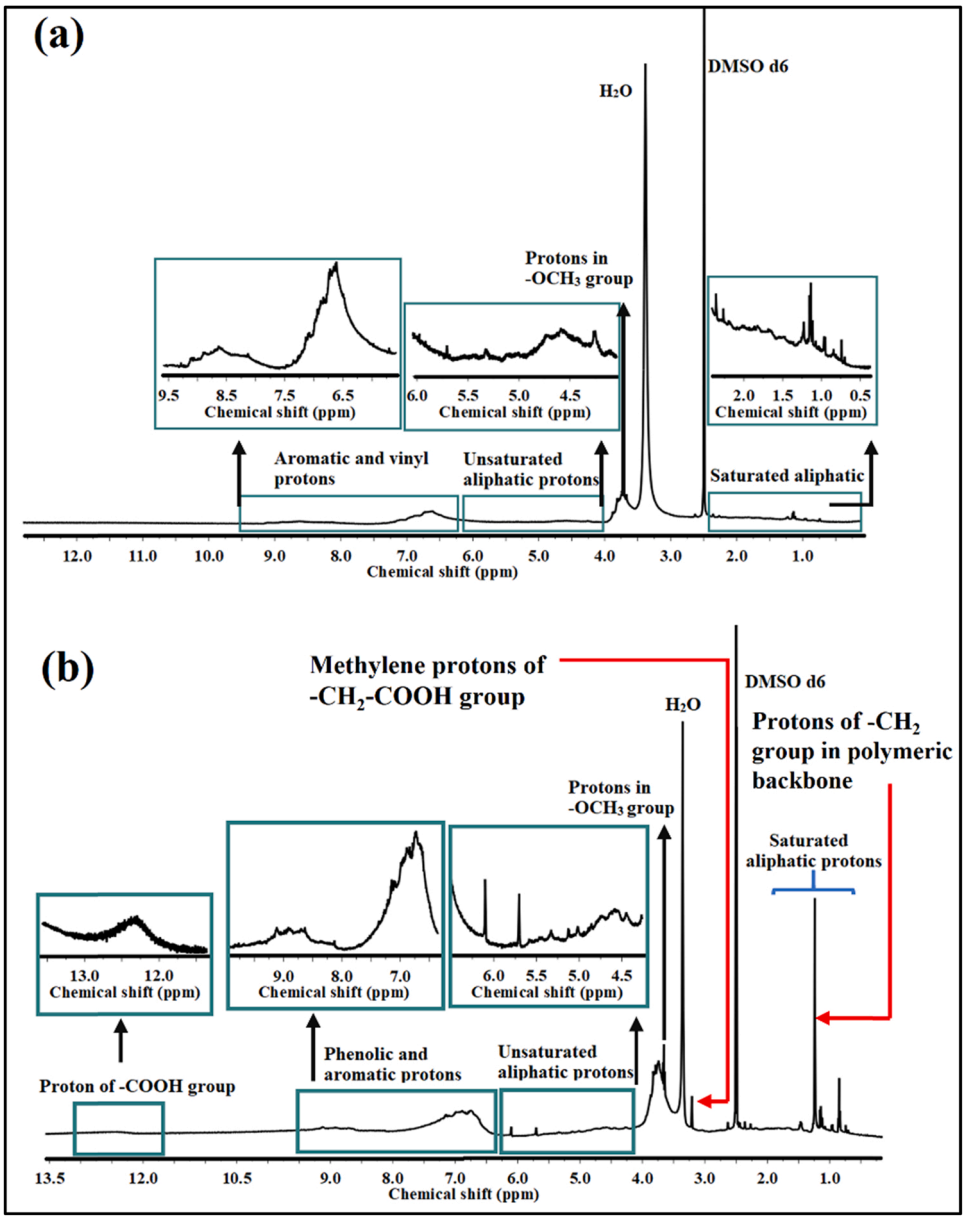

Fig. 4. (a and b) NMR spectra of lignin and P(IA)-f-lignin.

stretching of -O–C═O-/-C–OH (secondary alcohol) group, respectively. Similar kind of results ate observed in Pinto et al. (2013), Gadhave et al. (2020), Zhang et al. (2020). But after incorporation of different wt% P (IA)-f-Lignin, slight shifting is observed in the absorbance bands of PVAc with the addition of few new bands. For example, in lignin the O−H stretching found at 3410 cm^{-1} but there is a red shift (Fig. 6. b) of O−H stretching (3380 cm^{-1}) after incorporation of P(IA)-f-L and the right-hand shifting increases (3380 cm^{-1}→3373 cm^{-1}→3370 cm^{-1}) with the increase of loading. Such kind of phenomena is attributed to the increasing H-bonding with the polar functional groups of P(IA)-f-Lignin and PVAc (Lin et al., 2015). Signature bands for aromatic skeleton vibrations at 1595–1592, 1511, 1463 cm^{-1} clearly visible in the FTIR spectra of PVAc@P(IA)-f-L composite resins whereas such bands are absent in PVAc. Few other absorbance bands observed in FTIR spectra of the blends at 1371 cm^{-1} (-O-H deformation), 1226–1080 cm^{-1} (C–O stretching of -C–OH (primary/secondary alcohol)/-O–C═O- group), 1020 and 944 cm^{-1} (in plane and out of plane bending of aromatic C—H bond), 793, 629 and 604 cm^{-1} (C–H rocking vibration) are exactly same as PVAc (Wang et al., 2012; Wei et al., 2012).

3.5. Evaluation of viscosity

The change in viscosity of PVAc after incorporation of different wt% of P(IA)-f-Lignin was inspected using rheological study and corresponding viscosity vs shear rate curves are represented in Fig. 7. a. From, the curves it is confirmed that there is a significant change in the adhesive's rheological properties after inclusion of P(IA)-f-Lignin.

In case of PVAc the viscosity appears to decrease marginally when the shear rate increases, but it decreases sharply as the concentration of P(IA)-f-Lignin increases. In PVAc, the obtained curve showed a quasi-Newtonian behavior throughout the shear range. Whereas after incorporation of P(IA)-f-Lignin, all the curves showed a Newtonian-plateau throughout the shear range. Such anomalous behavior corresponds to the shear thinning effect (Pinto et al., 2013). Upon employment of shear rate on PVAc@P(IA)-f-L-20, disentanglement takes place between PVAc and P(IA)-f-Lignin which dramatically reduces the intramolecular interaction and results in the removal of entrapped water (Chaabouni and Boufi, 2017). As a result, a decreasing trend in viscosity is observed as the shear rate increases. However, such shear thinning effect

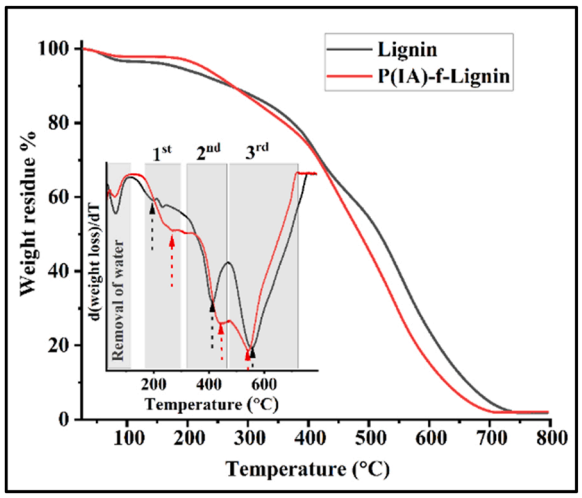

Fig. 5. TGA thermograms and their DTG curves (inset) of lignin and P(IA)-f-Lignin.

increases with the increasing concentration of P(IA)-f-Lignin moiety which result in sharp decrease in viscosity in lower shear rate. Most interestingly, the viscosity increases gradually (Table 1) from PVAc to PVAc@P(IA)-f-L-20→PVAc@P(IA)-f-L-30→PVAc@P(IA)-f-L-40 which is attributed to increasing solid content from 44 wt% to 49.09 wt%→ 53.3 wt%→ 56.92 wt% as well as increasing secondary interactions.

Furthermore, the change in other viscoelastic properties (storage modulus and tan δ) with temperature were shown in Fig. 7. b & c. The obtained results confirmed an increasing trend in storage modulus and a decreasing trend in tan δ intensity with temperature. Results are very much similar with López-Suevos et al. (2010), Chaabouni and Boufi (2017), Zhang et al. (2018). Reinforcement factor (R_f) of the blends were evaluated by dividing each composite's storage modulus by the storage modulus of pure PVAc at a particular temperature (0 °C and 80 °C). From the tabulated results (Table 1) it is evident that R_f value of the composites increases drastically after loading of P(IA)-f-Lignin. Such increasing trend in R_f values correspond to homogenous dispersion of P (IA)-f-Lignin in PVAc as well as the presence of extensive secondary interactions (especially hydrogen bonding) in between functionalized lignin and PVAc (Kaboorani and Riedl, 2011).

On the other hand, presence of P(IA)-f-Lignin minimizes the intensity of the tan δ peak (from 1.24 to 1.02→0.96→1.0) slightly compared to pure PVAc (Fig. 7. c). Such kind of phenomena of the composites might be due to the restricted segmental mobility of PVAc chains in presence of P(IA)-f-Lignin (Chaabouni and Boufi, 2017). Presence of strong H-bonding interaction between –COOH group of P(IA)-f-Lignin and acetyl group of vinyl acetate result in a highly stable intricated structure in the composite resin. Higher the amount of functionalized lignin in the composites, stronger will be the extent of secondary interactions. Which significantly reduces the segmental motion of PVAc chains and results in a slight shifting of tan δ peak to a higher temperature. The minimal shift of tan δ peak in PVAc@P(IA)-f-L-40 owing to a stronger intramolecular interaction between functionalized lignin moieties which somehow greater than interfacial interaction between functionalized lignin and PVAc.

3.6. Thermal stability analysis

TGA curves and their first derivative thermograms (DTG) of PVAc and their compositions were displayed in Fig. 7. d. TGA was employed to inspect the change in thermal stability after incorporation of various amount of P(IA)-f-Lignin in PVAc. All the formulated compositions showed multi-step degradation pattern (Kaboorani and Riedl, 2012; Zhang et al., 2020). The initial degradation starts from 170 to 280 °C which corresponds to the evaporation of trapped water molecule. The second step degradation founds in the range of 280–410 °C (PDT: 351 °C) which is mainly due to the degradation of PVAc backbone (Kaboorani et al., 2012). Mainly this type of degradation underwent through thermo-cracking of C—C and C—O bond. Noticeably, the intensity of degradation peak slightly decreases with the increasing amount of P(IA)-f-Lignin. This might be due to enhanced thermal stability of P(IA)-f-Lignin. As a result, the amount of weight residue at this particular temperature increases gradually like PVAc(58.7 %)→ PVAc@P(IA)-f-L-20(60.98 %)→ PVAc@P(IA)-f-L-30(62.32 %)→ PVAc @P(IA)-f-L-40(64.22 %). Third step degradation in the range of 410–500 °C (PDT: 434–444 °C) assigns to depolymerization reaction of P(IA)-f-Lignin. In this step lignin degraded into phenols/polyphenolic compounds through chain scission reaction. In forth step of degradation, these polyphenolic compound produces inert char layer through carbonization reaction. Most interestingly, the amount of char produced in PVAc after the degradation process is about 1.5 wt% whereas the amount of char increases gradually (PVAc@P(IA)-f-L-20 (8.23 %)→ PVAc@P(IA)-f-L-30 (15.53 %)→PVAc@P(IA)-f-L-40 (18,93 %)) with the increasing amount of P(IA)-f-Lignin. This is owing to lignin's carbonization property and improved physico-chemical interaction (Zhang et al., 2020).

3.7. Evaluation of adhesive properties

Fig. 8. (a) shows the adhesion strength of wood joints formed in the ambient temperature condition with PVAc and PVAc@P(IA)-f-L composite resins at various P(IA)-f-Lignin concentrations. Average lap shear strength of all the samples is presented in Table 1.

It is corroborated by the tabulated data that the addition of P(IA)-f-

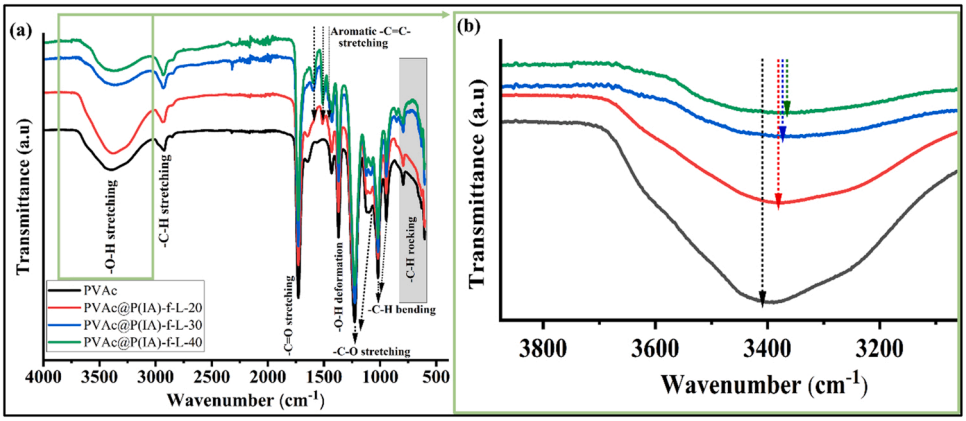

Fig. 6. FTIR spectra of (a) PVAc and PVAc@P(IA)-f-L composite resins and (b) represents the expanded region of the FTIR spectra.

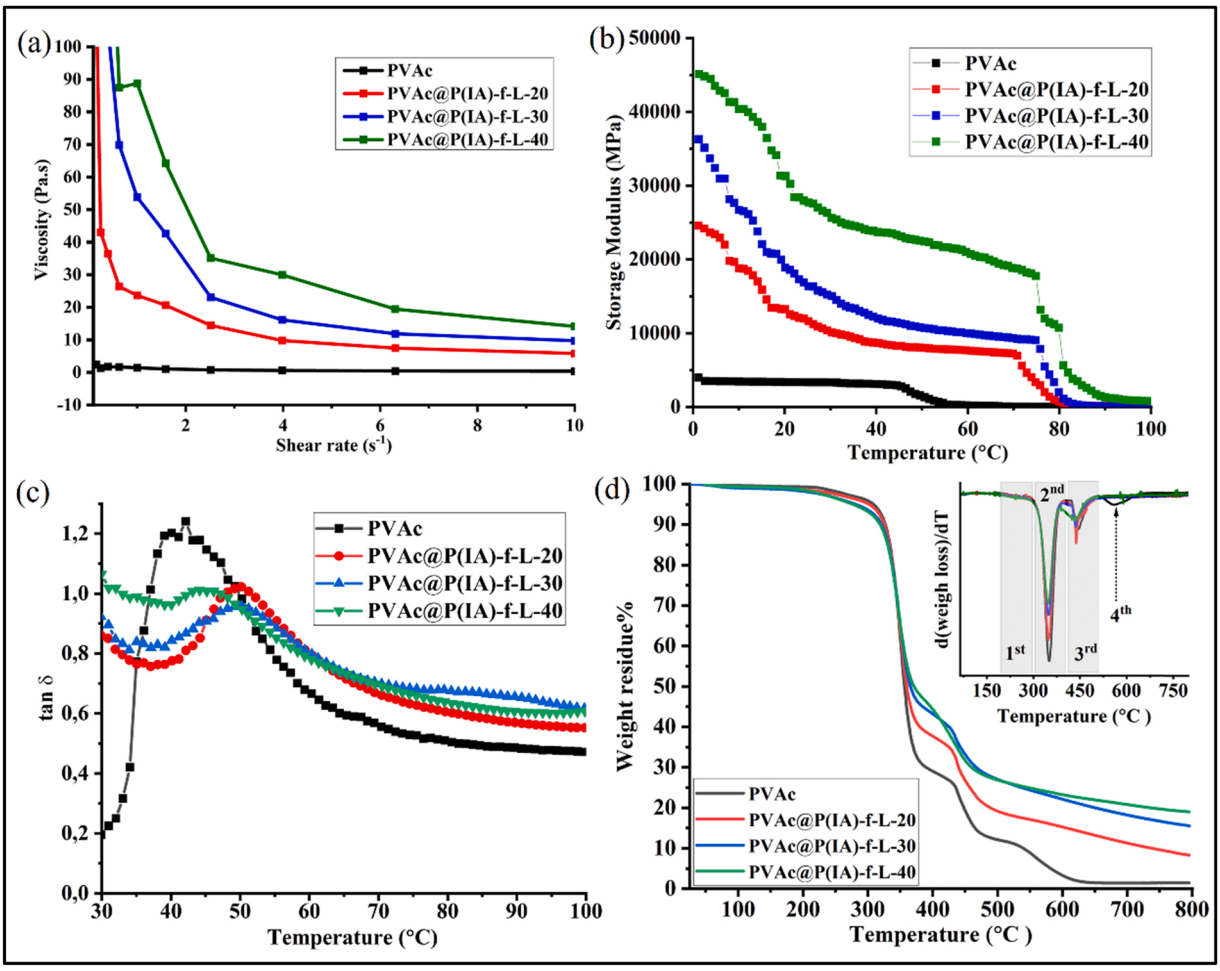

Fig. 7. (a) Viscosity vs. shear rate curve, (b) storage modulus vs temperature curve, (c) tan δ vs temperature curve, and (d) TGA and DTG (inset) thermograms of PVAc and PVAc@P(IA)-f-L composite resins.

Table 1
Solid content, various rheological parameters, shear strength of PVAc and PVAc@P(IA)-f-L blends.

Parameters	PVAc	PVAc@P (IA)-f-L-20	PVAc@P (IA)-f-L-30	PVAc@P (IA)-f-L-40
Solid content (%)	44	49.09	53.3	56.92
Viscosity[a] (Pa s) at 2 s^{-1} shear rate	0.2	18	35	53
Storage modulus at 0 °C (MPa)	3988	25,492	36,305	45,113
R_f (0 °C)	1	6.3	9.1	11.3
Storage modulus at 80 °C (MPa)	20.19	742	1865	9938
R_f (80 °C)	1	3.6	92.3	492.2
Shear strength[b] (MPa)	3.32 ± 0.12	4.62 ± 0.33	5.47 ± 0.10	7.83 ± 0.45
Shear strength[c] (MPa)	0.48 ± 0.20	1.90 ± 0.10	4.78 ± 0.25	5.17 ± 0.20

[a] Viscosity (Pa s) is measured at shear rate of (10 s^{-1}) at 25 °C.
[b] Shear strength in dry state (after drying 12 h in 25 °C).
[c] Shear strength after 6 h immersion in water followed by re-drying.

Lignin causes a significant change in shear strength. Obtained lap shear strength for the PVAc in dry state is near about 3.32 MPa whereas the shear strength is 4.62 MPa after loading of 20 wt% P(IA)-f-L. Moreover, a dose dependent behavior is overserved for all the formulated samples which resembles with prior art reports (Jiang et al., 2018; Kaboorani and Riedl, 2012; Khan et al., 2013). For example, with the increase in loading of P(IA)-f-Lignin from 20 to 30–40 wt% in PVAc, shear strength increases progressively from 4.62 MPa to 5.46–7.83 MPa. In general, the physico-chemical interlocking mechanism determines the adhesive property of the wooden substrate (Todorovic et al., 2021). Mainly, the surface of the wood comprised of extensive amount of polar functional groups (-OH groups of cellulose, hemicellulose) along with lot of micro-pores (Ghosh et al., 2020). Thus, when PVAc is applied on the wooden surface, it flows in between the micropores. After diffusion of the adhesive into the micropores, the polar components of PVAc establishes strong secondary interaction (H-bonding and van der Waals interaction) with the cellulosic counterparts (mainly with the -OH group) of wood. The amount of interaction gradually increases with the evaporation of water and consecutive solidification of PVAc. This kind of secondary interactions reach to its optimum limit upon complete evaporation of the water from the PVAc emulsion. As a result, the applied PVAc adhesive physically interlocked in between the wooden substrate and creates a mechanically rigid glue line. Thus, when stress is applied during a lap-shear test, the strong glue line prevents the wooden substrate from being separated. Most of the cases separation occurs through wood failure (as shown in the digital images of Fig. 8b) because the bonding strength in glue line is greater than the strength of the wooden substrate (Kaboorani et al., 2012). As mentioned in the earlier section, that there is an increasing trend in adhesive properties. This is due to the unique structural features of P(IA)-f-Lignin which contains extensive number of polar functional groups (-OH, -COOH, ester groups). Higher amount of polar functional groups results in extensive amount of secondary interactions (as shown in Scheme 2) which

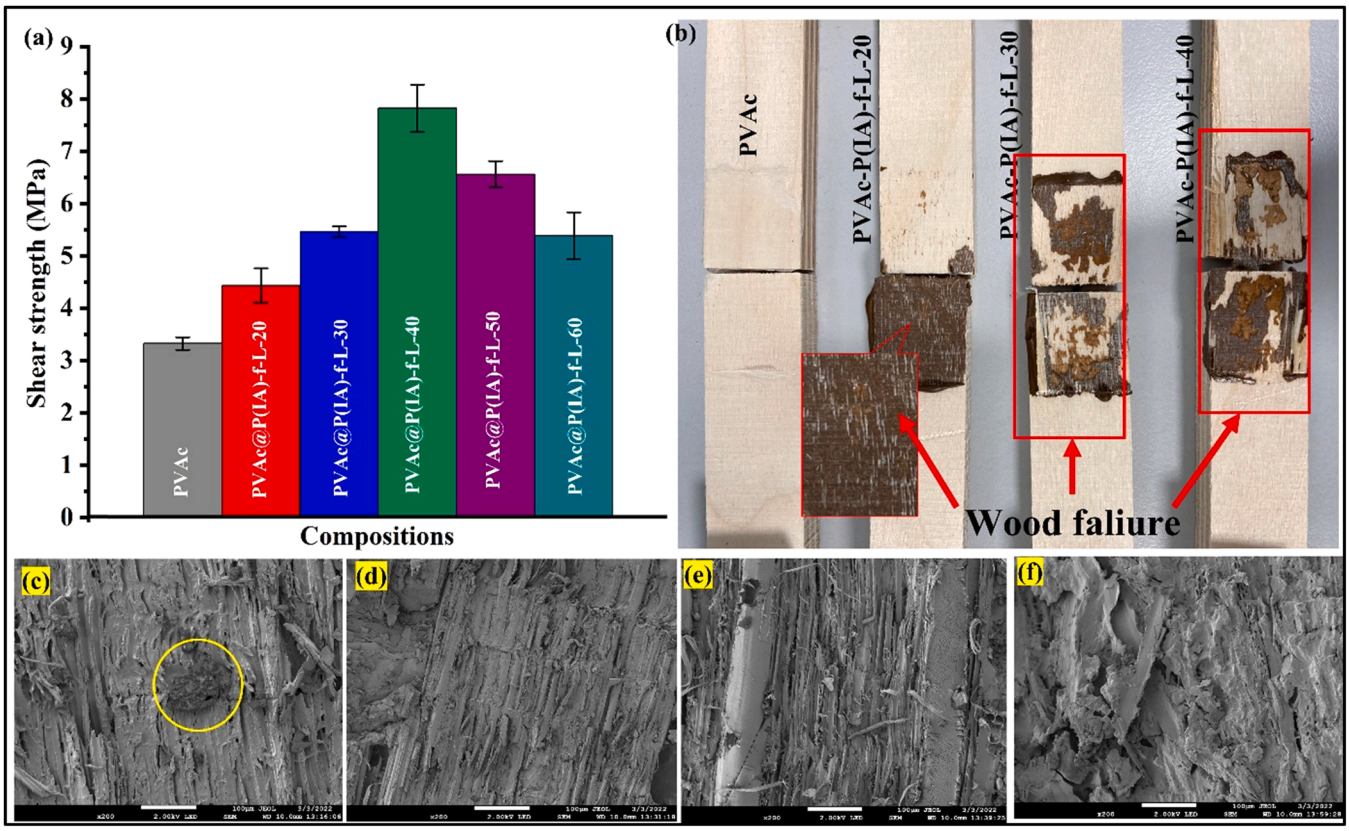

Fig. 8. (a) Shear strength of PVAc and PVAc@P(IA)-f-L composite resin, (b) digital images and (c–f) SEM images of mechanically fractured wooden surfaces.

indirectly enhances the physico-chemical interaction with the wooden substrate (Jiang et al., 2018). Moreover, the aromatic structures present in the lignin moiety of P(IA)-f-Lignin helps to minimize the applied the stress during the experiment. Higher the amount of P(IA)-f-Lignin, higher will be stress transfer. Combined attribute of both these factors are the main reason for such increasing lap-shear strength.

However, SEM images (Fig. 8. c–f) of mechanically damaged wood surfaces were examined to understand the fracture mechanics of the manufactured composite resins. From Fig. 8. c (fractured surface of PVAc glued wooden surface) it is evident that crack propagation initiates both from wood lumen as well as the adhesive layers. Some parts of the fractured surface contain thin film of PVAc resin (marked with yellow circle). Henceforth, the resultant morphology is a combined attribute of both wood and adhesive layer failure (Wang et al., 2012). Whereas in the SEM images of composite resins (Fig. 8. d–f), crack propagation starts from wooden lumen. No trace of composite resins can be seen across the shattered surfaces. Wooden lumens are uprooted throughout the fractured surface and such kind of phenomena increases with the increase of functionalized lignin content in PVAc matrix (Khan et al., 2013). Increasing physico-mechanical interlocking of the composite resins with wooden surface is responsible for such morphology. The formed glue line in the bonded joint is comparatively stronger than the wooden lumens. Therefore, at high shear value wood failure occurs in place of adhesive failure.

It is very important to mention that PVAc emulsion with 40 wt% of P(IA)-f-Lignin showed optimum adhesion strength. After that shear strength decreases gradually with the increasing content of functionalized lignin. Shear strength values for PVAc@P(IA)-f-L-50 and PVAc@P(IA)-f-L-60 are 6.57 ± 0.25 and 5.39 ± 0.45, respectively. This might be due to the increasing intermolecular interaction in between P(IA)-f-Lignin which creates unwanted agglomeration in PVAc-based composite resins. As a result, pre-mature failure occurs during lap shear strength. Moreover, the lap shear strength values of the composite resins in 'wet-redry' state is also represented in Table 1. According to the tabulated results, the composite resins demonstrated considerably better properties than pure PVAc. This might be due to the generation of extensive number of secondary interactions which directly enhance the physical crosslinking in composite resin, resulting in a significant increase in water resistance property (Todorovic et al., 2021; Wang et al., 2012). Surprisingly, the results are very much superior to the prior art reports in terms of renewability and adhesive strength. A comparison data is provided in Table 2 for better understanding.

4. Conclusion

In conclusion, we have successfully synthesized a P(IA)-f-Lignin by simple free radical polymerization of a partially neutralized IA acid monomer from the lignin surface that has very good compatibility with PVAc resin. The obtained P(IA)-f-Lignin was characterized by zeta potential, FTIR NMR, FESEM and TGA techniques. The P(IA) of P(IA)-f-Lignin has di carboxyl group on the surface and therefore the P(IA)-f-Lignin has very good scope to produce various types of advanced composite materials with waterborne polymers. Here, we report a novel method for successful preparation of PVAc@P(IA)-f-L composite resin for the first time with high lignin content for wood adhesive application by simple blending of P(IA)-f-Lignin (20, 30, 40, 50, and 60 wt%) with aqueous emulsion of PVAc. The FTIR spectroscopy, TGA and viscosity analysis confirm the successful integration of high concentration of P(IA)-f-L into the aqueous emulsion of PVAc. The H-bonding interaction between oxygen containing functional group of PVAc (-OH and ester) and oxygen containing functional groups of P(IA)-f-Lignin (-OH and -COOH) govern the chemistry of compatibilization of P(IA)-f-Lignin with PVAc in the composite resin. The PVAc@P(IA)-f-L composite resins showed significant enhancement in wood adhesion strength compared to pure PVAc resin. The PVAc@P(IA)-f-L40 composite resins showed significant wood adhesion strength of 7.83 ± 0.45 MPa which is

Table 2
Comparison table of adhesive strengths with prior art reports.

SL. no.	Major components	Adhesive properties for the best compositions	Ref.
1.	Acetonitrile extracting lignin + phenol + polyvinylpyrrolidone (K30)	1.70 MPa	Gong et al. (2020)
2.	Ozonated lignin (Oz-L) + sebacic acid-derived epoxy (Se-EP) + zinc catalyst (Zn $(acac)_2$)	~ 13 MPa	Zhang et al. (2018)
3.	Kraft lignin and glycerol diglycidyl ether	2.0–2.5 MPa	Li et al. (2018)
4.	Lignin-vinyl acetate copolymer	Tensile strength of lignin coated paper increases 1.86 times	Z. Zhang et al. (2021), N. Zhang et al. (2021) (Zhang et al., 2020)
5.	Poly(vinylacetate)-cellulose nanofibril based adhesive Starch- cellulose nanofibril based adhesive	10–11 MPa 7–8 MPa	Jiang et al. (2018)
6.	Graphene-poly(vinylacetate) based adhesive	2.0–2.5 MPa	Khan et al. (2013)
7.	Nano clay-poly(vinylacetate) based adhesive	10–20 % increase after loading of nanoclay	Kaboorani and Riedl (2011)
8.	Cellulose nanofibrils-poly(vinylacetate) based adhesives	8.12 MPa	Chaabouni and Boufi (2017)
9.	Starch- poly(vinylacetate) based adhesives	4.45 MPa	Wang et al. (2012)
10.	**PVAc@P(IA)-f-L-40**	**7.83 MPa**	**Current report**

2.35 times higher compared to compared to pure PVAc resin (3.32 ± 0.12 MPa). The significant improved wood adhesion strength of the PVAc@P(IA)-f-L composites resin with high quantity of lignin content is very promising to reduce the cost as well as enhancement of sustainability PVAc based wood adhesive. Based on the prior art reports on lignin-based adhesive, we anticipate that the current study provides a new paradigm in the production of adhesive using substantial amount of lignin. This not only removes the obstacle of lignin use, but also reduces the cost of production and the non-renewability issues in fossil fuel-based adhesives.

Declaration of Competing Interest

The authors declare that they have no known competing financial interests or personal relationships that could have appeared to influence the work reported in this paper.

Data Availability

Data will be made available on request.

Acknowledgements

This work was supported by the Seed grant of MEC pilot, Finland through IIT-LUT collaboration and Kollin säätiö funding for biorefinery research of LUT University, Lahti campus, Finland.

Author Statement

- ➢ The work reported in the submitted manuscript has not been published previously and is not under consideration for publication elsewhere.
- ➢ This manuscript has not been considered previously by Industrial Crops and Products.
- ➢ This is also to inform that there is no actual or potential conflict of interest including any financial, personal, or other relationships with other people or organizations that could inappropriately influence or be perceived to influence this work.

References

Baş, G.S., Sancaktar, E., 2020. Mechanical behavior of toughened epoxy structural adhesives for impact applications. ChemEngineering 4, 38. https://doi.org/10.3390/chemengineering4020038.

Bednarz, S., Błaszczyk, A., Błazejewska, D., Bogdał, D., 2015. Free-radical polymerization of itaconic acid in the presence of choline salts: mechanism of persulfate decomposition. Catal. Today 257, 297–304. https://doi.org/10.1016/j.cattod.2014.07.021.

Chaabouni, O., Boufi, S., 2017. Cellulose nanofibrils/polyvinyl acetate nanocomposite adhesives with improved mechanical properties. Carbohydr. Polym. 156, 64–70. https://doi.org/10.1016/j.carbpol.2016.09.016.

Cottet, C., Salvay, A.G., Peltzer, M.A., Fernández-García, M., 2021. Incorporation of poly (Itaconic acid) with quaternized thiazole groups on gelatin-based films for antimicrobial-active food packaging. Polymers 13, 1–21. https://doi.org/10.3390/polym13020200.

Crouvisier-Urion, K., Regina Da Silva Farias, F., Arunatat, S., Griffin, D., Gerometta, M., Rocca-Smith, J.R., Weber, G., Sok, N., Karbowiak, T., 2019. Functionalization of chitosan with lignin to produce active materials by waste valorization. Green Chem. 21, 4633–4641. https://doi.org/10.1039/c9gc01372e.

Dinte, E., Sylvester, B., 2018. Adhesives: applications and recent advances. In: Applied Adhesive Bonding in Science and Technology. InTech. https://doi.org/10.5772/intechopen.71854.

Gadhave, R.v., Mahanwar, P.A., Gadekar, P.T., Kasbe, P.S., 2020. A study on the effect of starch–polyvinyl alcohol blends by addition of citric acid and boric acid for enhancement in performance properties of polyvinyl acetate-based wood adhesive. J. Indian Acad. Wood Sci. 17, 9–20. https://doi.org/10.1007/s13196-019-00249-6.

Ghosh, T., Voit, B., Karak, N., 2020. Polystyrene/thermoplastic polyurethane interpenetrating network-based nanocomposite with high-speed, thermo-responsive shape memory behavior. Polymer 200, 122575. https://doi.org/10.1016/j.polymer.2020.122575.

Gong, X., Liu, T., Yu, S., Meng, Y., Lu, J., Cheng, Y., Wang, H., 2020. The preparation and performance of a novel lignin-based adhesive without formaldehyde. Ind. Crops Prod. 153. https://doi.org/10.1016/j.indcrop.2020.112593.

Jiang, W., Tomppo, L., Pakarinen, T., Sirviö, J.A., Liimatainen, H., Haapala, A., 2018. Effect of cellulose nanofibrils on the bond strength of polyvinyl acetate and starch adhesives for wood. BioResources 13, 2283–2292. https://doi.org/10.15376/biores.13.2.2283-2292.

Kaboorani, A., Riedl, B., 2011. Effects of adding nano-clay on performance of polyvinyl acetate (PVA) as a wood adhesive. Compos. Part A: Appl. Sci. Manuf. 42, 1031–1039. https://doi.org/10.1016/j.compositesa.2011.04.007.

Kaboorani, A., Riedl, B., 2012. Nano-aluminum oxide as a reinforcing material for thermoplastic adhesives. J. Ind. Eng. Chem. 18, 1076–1081. https://doi.org/10.1016/j.jiec.2011.12.001.

Kaboorani, A., Riedl, B., Blanchet, P., Fellin, M., Hosseinaei, O., Wang, S., 2012. Nanocrystalline cellulose (NCC): a renewable nano-material for polyvinyl acetate (PVA) adhesive. Eur. Polym. J. 48, 1829–1837. https://doi.org/10.1016/j.eurpolymj.2012.08.008.

Kaur, R., Thakur, N.S., Chandna, S., Bhaumik, J., 2021. Sustainable lignin-based coatings doped with titanium dioxide nanocomposites exhibit synergistic microbicidal and UV-blocking performance toward personal protective equipment. ACS Sustain. Chem. Eng. 9, 11223–11237. https://doi.org/10.1021/acssuschemeng.1c03637.

Khan, U., May, P., Porwal, H., Nawaz, K., Coleman, J.N., 2013. Improved adhesive strength and toughness of polyvinyl acetate glue on addition of small quantities of graphene. ACS Appl. Mater. Interfaces 5, 1423–1428. https://doi.org/10.1021/am302864f.

Kollman, M., Jiang, X., Thompson, S.J., Mante, O., Dayton, D.C., Chang, H.M., Jameel, H., 2021. Improved understanding of technical lignin functionalization through comprehensive structural characterization of fractionated pine kraft lignins modified by the Mannich reaction. Green Chem. 23, 7122–7136. https://doi.org/10.1039/d1gc01842f.

Kumar, A., Sood, A., Han, S.S., 2022. Potential of magnetic nanocellulose in biomedical applications: recent advances. Biomater. Polym. Horiz. 1, 32–47. https://doi.org/10.37819/bph.001.01.0133.

Li, R.J., Gutierrez, J., Chung, Y.L., Frank, C.W., Billington, S.L., Sattely, E.S., 2018. A lignin-epoxy resin derived from biomass as an alternative to formaldehyde-based wood adhesives. Green Chem. 20, 1459–1466. https://doi.org/10.1039/c7gc03026f.

Lin, Y., Liu, L., Xu, G., Zhang, D., Guan, A., Wu, G., 2015. Interfacial interactions and segmental dynamics of poly(vinyl acetate)/silica nanocomposites. J. Phys. Chem. C 119, 12956–12966. https://doi.org/10.1021/acs.jpcc.5b01240.

López-Suevos, F., Eyholzer, C., Bordeanu, N., Richter, K., 2010. DMA analysis and wood bonding of PVAc latex reinforced with cellulose nanofibrils. ⟨https://doi.org/10.3929/ethz-b-000018260⟩.

Maksimov, R.D., Bitenieks, J., Plume, E., Zicans, J., Merijs Meri, R., 2010. The effect of introduction of carbon nanotubes on the physicomechanical properties of polyvinylacetate.

Manara, P., Zabaniotou, A., Vanderghem, C., Richel, A., 2014. Lignin extraction from Mediterranean agro-wastes: impact of pretreatment conditions on lignin chemical structure and thermal degradation behavior. Catal. Today 25–34. https://doi.org/10.1016/j.cattod.2013.10.065.

Myint, A.A., Lee, H.W., Seo, B., Son, W.S., Yoon, Junho, Yoon, T.J., Park, H.J., Yu, J., Yoon, Jeyong, Lee, Y.W., 2016. One pot synthesis of environmentally friendly lignin nanoparticles with compressed liquid carbon dioxide as an antisolvent. Green Chem. 18, 2129–2146. https://doi.org/10.1039/c5gc02398j.

Panesar, S.S., Jacob, S., Misra, M., Mohanty, A.K., 2013. Functionalization of lignin: fundamental studies on aqueous graft copolymerization with vinyl acetate. Ind. Crops Prod. 46, 191–196. https://doi.org/10.1016/j.indcrop.2012.12.031.

Pei, W., Shang, W., Liang, C., Jiang, X., Huang, C., Yong, Q., 2020. Using lignin as the precursor to synthesize Fe3O4@lignin composite for preparing electromagnetic wave absorbing lignin-phenol-formaldehyde adhesive. Ind. Crops Prod. 154. https://doi.org/10.1016/j.indcrop.2020.112638.

Pinto, A.M., Martins, J., Moreira, J.A., Mendes, A.M., Magalhães, F.D., 2013. Dispersion of graphene nanoplatelets in poly(vinyl acetate) latex and effect on adhesive bond strength. Polym. Int. 62, 928–935. https://doi.org/10.1002/pi.4379.

Rana, A.K., Frollini, E., Thakur, V.K., 2021a. Cellulose nanocrystals: pretreatments, preparation strategies, and surface functionalization. Int. J. Biol. Macromol. https://doi.org/10.1016/j.ijbiomac.2021.05.119.

Rana, A.K., Potluri, P., Thakur, V.K., 2021c. Cellulosic grewia optiva fibres: towards chemistry, surface engineering and sustainable materials. J. Environ. Chem. Eng. 182, 1554–1581. https://doi.org/10.1016/j.jece.2021.106059.

Rana, A.K., Gupta, V.K., Saini, A.K., Voicu, S.I., Abdellattifaand, M.H., Thakur, V.K., 2021b. Water desalination using nanocelluloses/cellulose derivatives based membranes for sustainable future. Desalination 520. https://doi.org/10.1016/j.desal.2021.115359.

Rezania, H., Vatanpour, V., Faghani, S., 2019. Poly(itaconic acid)-assisted ultrafiltration of heavy metal ions' removal from wastewater. Iran. Polym. J. (Engl. Ed.) 28, 1069–1077. https://doi.org/10.1007/s13726-019-00767-7.

Salthammer, T., Mentese, S., Marutzky, R., 2010. Formaldehyde in the indoor environment. Chem. Rev. 110, 2536–2572. https://doi.org/10.1021/cr800399g.

Sánchez-Valdes, S., Ramírez-Vargas, E., Ibarra-Alonso, M.C., Ramos De Valle, L.F., Méndez-Nonell, J., Medellín-Rodríguez, F.J., Martínez-Colunga, J.G., Vazquez-Rodriguez, S., Betancourt-Galindo, R., 2012. Itaconic acid and amino alcohol functionalized polyethylene as compatibilizers for polyethylene nanocomposites. Compos. Part B: Eng. 43, 497–502. https://doi.org/10.1016/j.compositesb.2011.08.018.

Shu, Y., Luo, Q., Wang, M., Ouyang, Y., Lin, H., Sheng, L., Su, S., 2021. Preparation and properties of poly(lactic acid)/lignin-modified polyvinyl acetate composites. J. Appl. Polym. Sci. 138. https://doi.org/10.1002/app.49844.

Song, X., Zhang, L., Wang, Y., Zhao, R., Sun, X., Tian, Y., Sun, R., Hua, C., Bai, R., Wang, C., Gao, S., 2022. Long term antibacterial effect cellulose film was modified with polyhexamethylene biguanide (PHMB). Ind. Crops Prod. 184, 115038 https://doi.org/10.1016/j.indcrop.2022.115038.

Todorovic, T., Norström, E., Khabbaz, F., Brücher, J., Malmström, E., Fogelström, L., 2021. A fully bio-based wood adhesive valorising hemicellulose-rich sidestreams from the pulp industry. Green Chem. 23, 3322–3333. https://doi.org/10.1039/d0gc04273k.

Tomić, S.L., Filipović, J.M., 2004. Synthesis and characterization of complexes between poly(itaconic acid) and poly(ethylene glycol). Polym. Bull. 52, 355–364. https://doi.org/10.1007/s00289-004-0298-5.

Uppal, N., Pappu, A., Gowri, V.K.S., Thakur, V.K., 2022. Cellulosic fibres-based epoxy composites: from bioresources to a circular economy. Ind. Crops Prod. 182, 114895 https://doi.org/10.1016/j.indcrop.2022.114895.

Wang, S., Hu, Z., Shi, J., Chen, G., Zhang, Q., Weng, Z., Wu, K., Lu, M., 2019. Green synthesis of graphene with the assistance of modified lignin and its application in anticorrosive waterborne epoxy coatings. Appl. Surf. Sci. 484, 759–770. https://doi.org/10.1016/j.apsusc.2019.03.229.

Wang, Z., Li, Z., Gu, Z., Hong, Y., Cheng, L., 2012. Preparation, characterization and properties of starch-based wood adhesive. Carbohydr. Polym. 88, 699–706. https://doi.org/10.1016/j.carbpol.2012.01.023.

Wei, S., Pintus, V., Schreiner, M., 2012. Photochemical degradation study of polyvinyl acetate paints used in artworks by Py-GC/MS. J. Anal. Appl. Pyrolysis 97, 158–163. https://doi.org/10.1016/j.jaap.2012.05.004.

Yan, P., Xu, Z., Zhang, C., Liu, X., Xu, W., Zhang, Z.C., 2015. Fractionation of lignin from eucalyptus bark using amine-sulfonate functionalized ionic liquids. Green Chem. 17, 4913–4920. https://doi.org/10.1039/c5gc01035g.

Yang, J., Gunasekaran, S., 2013. Electrochemically reduced graphene oxide sheets for use in high performance supercapacitors. Carbon 51, 36–44. https://doi.org/10.1016/j.carbon.2012.08.003.

Yu, Y., Fu, S., Song, P., Luo, X., Jin, Y., Lu, F., Wu, Q., Ye, J., 2012. Functionalized lignin by grafting phosphorus-nitrogen improves the thermal stability and flame retardancy of polypropylene. Polym. Degrad. Stab. 97, 541–546. https://doi.org/10.1016/j.polymdegradstab.2012.01.020.

Zhang, N., Wang, S., Gibril, M.E., Kong, F., 2020. The copolymer of polyvinyl acetate containing lignin-vinyl acetate monomer: synthesis and characterization. Eur. Polym. J. 123. https://doi.org/10.1016/j.eurpolymj.2019.109411.

Zhang, N., Liu, P., Yi, Y., Gibril, M.E., Wang, S., Kong, F., 2021. Application of polyvinyl acetate/lignin copolymer as bio-based coating material and its effects on paper properties. Coatings 11, 1–12. https://doi.org/10.3390/coatings11020192.

Zhang, S., Liu, T., Hao, C., Wang, L., Han, J., Liu, H., Zhang, J., 2018. Preparation of a lignin-based vitrimer material and its potential use for recoverable adhesives. Green Chem. 20, 2995–3000. https://doi.org/10.1039/c8gc01299g.

Zhang, Z., Terrasson, V., Guénin, E., 2021. Lignin nanoparticles and their nanocomposites. Nanomaterials 11, 1336. https://doi.org/10.3390/nano11051336.

Zong, E., Liu, X., Liu, L., Wang, J., Song, P., Ma, Z., Ding, J., Fu, S., 2018. Graft polymerization of acrylic monomers onto lignin with CaCl2-H2O2 as initiator: preparation, mechanism, characterization, and application in poly(lactic acid). ACS Sustain. Chem. Eng. 6, 337–348. https://doi.org/10.1021/acssuschemeng.7b02599.